# Solving Two-dimensional Forward Problems on an Annulus Using Spectral Fourier Methods

S. Choe
skchoe@cs.utah.edu

R. M. Kirby
kirby@cs.utah.edu

Jan 30th, 2004

**Abstract**

In this report, we present a spectral Fourier method for solving a Poisson equation with Dirichlet and Neumann boundary conditions respectively on an annulus domain. By using the tensor product between spectral and Fourier bases, we could apply the high-order method on the annulus domain. The fast Fourier transform allowed the rapid convergence on the radius to be maintained to all angular direction on the annulus.

## Contents

# 1 Introduction

Spectral method is a numerical scheme to approximate and simulate the solution of partial differential equations. It has developed rapidly in the past three decades and been applied to many field in numerical simulation.

One of main reasons that it has gained broad and fast acceptance is that it can take various system of infinitely differentiable basis functions as trial functions, for instance, we can use the representation of a function $u$ throughtout the domain via a truncated serier exansion as follows:

$$u \approx u_N = \sum_{n=0}^{N} \hat{u}_n \phi_n, \tag{1}$$

where $\phi_n$ are the basis functions. In general this basis functions may be the Chebyshev polynomials $T_n$ or the Legendre polynomials $L_n$ or another member of the class of Jacobi polynomials $P_n^{\alpha,\beta}$. By choosing an appropriate orthogonal system based on its domain of orthogonality, we can apply the method to problems such as periodic/non-periodic problems and problems defined on compact domain, half/all intervals.

Spectral methods can be classified into 2 parts in its characteristics. We call them to be nodal and modal method, respectively.

- The nodal method is usually called as pseudo-spectral or collocation methods. The coefficients $\hat{u}_n$ of (1) are obtained by requiring the residual function to be zero exactly at grid that is a set of nodes.

- The modal method is associated with the method of weighted residuals where the residual function is weighted with a set of test functions and after integration is set to zero. In our formulation we bring in the Galerkin method which has test functions same as the basis functions.

In the collocation approach the coefficients represent the nodal value of the physical variable unlike the Galerkin method.

The other thing which is so fascinating is its high accuracy and convergence. In particular, the spectral polynomial method facilitates the control of the resolution of element size and the order of approximation. This enables the method to converge in exponential speed which shows a noticeable difference from classical finite difference and other purely element methods. Unlike finite elements and finite difference, the order of convergence is not fixed and it is related to the maximum regularity of the solution.

In this report, I investigate the spectral polynomial method and Fourier method for solving a partial differential equation specific to the forward Poisson problem with Dirichlet and Neumann boundary condition on inner and outer boundary circles respectively. Throughout the report, I will formulate our approach that utilizes spectral polynomial element and Fourier method in tensor product form. As an conclusion we present the result of numerical solution and its convergence by h/p adaptive control.

# 2 The Numerical Solution of Poisson Equation on a 2-dimensional Annulus

## 2.1 Poisson Equation in Polar Coordinates and Basis Functions

We formulate the Generalized Poisson problem on an annulus $[a,b]\times[0,2\pi]$, $a>0$ under the periodic solution $u$ as follows:

$$-\left[\frac{\partial}{\partial r}(\sigma(r,\theta)\frac{\partial}{\partial r})+\frac{1}{r}(\sigma(r,\theta)\frac{\partial}{\partial r})+\frac{1}{r^2}\frac{\partial}{\partial\theta}(\sigma(r,\theta)\frac{\partial}{\partial\theta})\right]u(r,\theta)=f(r,\theta), \tag{2}$$

$$\text{with periodicity of } u,\quad u(r,0)=u(r,2\pi), \tag{3}$$

where $r\in[a,b]$ and $\theta\in[0,2\pi]$. The boundary conditions for this domain is given by

$$u(a,\theta)=\mathcal{G}_D(\theta),\qquad\qquad \frac{\partial}{\partial r}u(b,\theta)=\mathcal{G}_N(\theta), \tag{4}$$

where $\theta\in[0,2\pi]$.

The representation of approximation of $u$ is guaranteed by Weierstrass theorem:

$$u(r,\theta)=\sum_{j=0}^{N_r}\sum_{k=-N_\theta/2+1}^{N_\theta/2}\hat{u}_{jk}\phi_j(r)e^{ik\theta}, \tag{5}$$

where $r\in[a,b]$ and $\theta\in[0,2\pi]$ for the global degree of freedom $N_r$ and $N_\theta$ on $\hat{u}_{jk}$'s.

The basis function $\{\phi_j\}_{j=0}^{N_r}$ at (5) are defined as modified Jacobi polynomials defined in [1], [5].

As a review of discrete Fourier transform in $N$-point grid described in [2], the formula for the discrete Fourier transform for $\{v_j\}$ is

$$\hat{v}_k=h\sum_{j=1}^{N}e^{-ikx_j}v_j,\quad k=-\frac{N}{2}+1,\ldots,\frac{N}{2}, \tag{6}$$

where $x_j=j\frac{2\pi}{N}$ and the inverse discrete Fourier transform for $\{\hat{v}_k\}$ is given by

$$v_j=\frac{1}{2\pi}\sum_{k=-N/2+1}^{Nr/2}e^{ikx_j}\hat{v}_k,\quad j=1,\ldots,N. \tag{7}$$

## 2.2 Formulation of Spectral Polynomial and Fourier Methods

In this project, we assume the conductivity term $\sigma$ in (2) to be only dependent of variables showing the radius domain as we multiply $r^2$ in each side of (2). Then the Poisson equation and its modified form of polar coordinate was obtained as follows:

$$-\left[r^2\frac{\partial}{\partial r}(\sigma(r)\frac{\partial}{\partial r})+r\sigma(r)\frac{\partial}{\partial r}+\sigma(r)\frac{\partial^2}{\partial\theta^2}\right]u(r,\theta)=r^2f(r,\theta). \tag{8}$$

To apply Galerkin method, test functions are of the form:

$$\phi_p(r)e^{iq\theta}, \qquad p = 0, \ldots, N_r, \quad q = -\frac{N_\theta}{2} + 1, \ldots, \frac{N_\theta}{2}. \tag{9}$$

We have the weak form of the equation:

$$-\langle r^2 \frac{\partial}{\partial r}(\sigma \frac{\partial}{\partial r} u) + r\sigma \frac{\partial}{\partial r} u + \sigma \frac{\partial^2}{\partial \theta^2} u, \phi_p e^{iq\theta} \rangle = \langle r^2 f, \phi_p e^{iq\theta} \rangle. \tag{10}$$

Define $T_i, i = 1, \ldots, 4$ as follows

$$T_1 = \int_0^{2\pi} \int_a^b \phi_p e^{iq\theta} r^2 \frac{\partial}{\partial r} \left[ \sigma(r) \frac{\partial}{\partial r} u(r,\theta) \right] dr d\theta, \tag{11}$$

$$T_2 = \int_0^{2\pi} \int_a^b \phi_p e^{iq\theta} r\sigma(r) \frac{\partial}{\partial r} u(r,\theta) dr d\theta, \tag{12}$$

$$T_3 = \int_0^{2\pi} \int_a^b \phi_p e^{iq\theta} \sigma(r) \frac{\partial^2}{\partial \theta^2} u(r,\theta) dr d\theta, \tag{13}$$

and

$$T_4 = \int_0^{2\pi} \int_a^b \phi_p e^{iq\theta} r^2 f(r,\theta) dr d\theta \tag{14}$$

Then we can represent (10) to be:

$$-T_1 - T_2 - T_3 = T_4. \tag{15}$$

We can obtain boundary term by integration by part on $T_1$

$$T_1 = \int_0^{2\pi} e^{iq\theta} \left[ r^2 \sigma(r) \frac{\partial}{\partial r} u(r,\theta) \phi_p(r) \right]_a^b d\theta \tag{16}$$

$$- \; 2 \int_0^{2\pi} \int_a^b e^{iq\theta} r\sigma(r) \frac{\partial}{\partial r} u(r,\theta) \phi_p(r) dr d\theta \tag{17}$$

$$- \int_0^{2\pi} \int_a^b e^{iq\theta} r^2 \sigma(r) \frac{\partial}{\partial r} u(r,\theta) \frac{d}{dr} \phi_p(r) dr d\theta. \tag{18}$$

Then the right hand side of (15) becomes

$$-T_1 - T_2 - T_3 = -\int_0^{2\pi} e^{iq\theta} \left[ r^2 \sigma(r) \frac{\partial}{\partial r} u(r,\theta) \phi_p(r) \right]_a^b d\theta \tag{19}$$

$$+ \int_0^{2\pi} \int_a^b e^{iq\theta} r\sigma(r) \frac{\partial}{\partial r} u(r,\theta) \phi_p(r) dr d\theta \tag{20}$$

$$+ \int_0^{2\pi} \int_a^b e^{iq\theta} r^2 \sigma(r) \frac{\partial}{\partial r} u(r,\theta) \frac{d}{dr} \phi_p(r) dr d\theta \tag{21}$$

$$- \int_0^{2\pi} \int_a^b e^{iq\theta} \sigma(r) \frac{\partial^2}{\partial \theta^2} u(r,\theta) \phi_p(r) dr d\theta \tag{22}$$

By using (5) and the orthogonal property in $\{e^{ik\theta}\}k = -\frac{N_\theta}{2}+1,\ldots,\frac{N_\theta}{2}$, we can simplify (19) as follows:

$$
\begin{aligned}
-T_1 - T_2 - T_3 &= -\int_0^{2\pi} e^{iq\theta}\left[r^2\sigma(r)\frac{\partial}{\partial r}u(r,\theta)\phi_p(r)\right]_a^b d\theta && (23)\\
&+ 2\pi\sum_{j=0}^{N_\theta}\hat{u}_{jq}\int_a^b r\sigma(r)\frac{d}{dr}\phi_j(r)\phi_p(r)dr && (24)\\
&+ 2\pi\sum_{j=0}^{N_\theta}\hat{u}_{jq}\int_a^b r^2\sigma(r)\frac{d}{dr}\phi_j(r)\frac{d}{dr}\phi_p(r)dr && (25)\\
&+ 2\pi\sum_{j=0}^{N_\theta}\hat{u}_{jq}q^2\int_a^b \sigma(r)\phi_j(r)\phi_p(r)dr. && (26)
\end{aligned}
$$

Let us define the following matrices:

$$
\begin{aligned}
(\mathbf{M}_1)_{jp} &= \int_a^b r\sigma(r)\frac{d}{dr}\phi_j(r)\phi_p(r)\ dr && (27)\\
(\mathbf{M}_2)_{jp} &= \int_a^b r^2\sigma(r)\frac{d}{dr}\phi_j(r)\frac{d}{dr}\phi_p(r)\ dr && (28)\\
(\mathbf{M}_3)_{jp} &= \int_a^b \sigma(r)\phi_j(r)\phi_p(r)\ dr, && (29)
\end{aligned}
$$

where $j,p = 0,\ldots,N_\theta$.

Now the form $T_4$ is as follows.

$$
\begin{aligned}
T_4 &= \int_a^b\int_0^{2\pi}\phi_p(r)e^{iq\theta}r^2 f(r,\theta)d\theta dr && (30)\\
&= \int_a^b r^2\phi_p(r)\int_0^{2\pi} f(r,\theta)e^{iq\theta}d\theta dr && (31)\\
& && (32)
\end{aligned}
$$

For given $r$, the Discrete Fourier Transform for $f(r,\theta)$ is defined by

$$
f(r,\theta_\tau) = \frac{1}{2\pi}\sum_{k=-N_\theta/2+1}^{N_\theta/2} e^{ik\theta_\tau}\widehat{f(r)}_k \qquad (33)
$$

where

$$
\widehat{f(r)}_k = \frac{2\pi}{N_\theta}\sum_{j=1}^{N_\theta} e^{-ik\theta_j}f(r,\theta_j) \qquad (34)
$$

with $k \in \{-\frac{N_\theta}{2}+1,\cdots,\frac{N_\theta}{2}\}$ and $\theta_j \in \{\frac{2\pi}{N_\theta},\cdots,2\pi\}$.

Then

$$T_4 = \int_a^b r^2 \phi_p(r) \int_0^{2\pi} \frac{1}{2\pi} \sum_{k=-N_\theta/2+1}^{N_\theta/2} e^{ik\theta} \widehat{f(r)}_k e^{iq\theta} d\theta dr \tag{35}$$

$$= \int_a^b r^2 \phi_p(r) \widehat{f(r)}_q dr. \tag{36}$$

Since we have this relation $-T_1 - T_2 - T_3 = T_4$,

$$2\pi \sum_{j=0}^{N_\theta} \hat{u}_{jq} M_{1\,jp} + 2\pi \sum_{j=0}^{N_\theta} \hat{u}_{jq} M_{2jp} + 2\pi \sum_{j=0}^{N_\theta} \hat{u}_{jq} q^2 M_{3jp} = \int_a^b r^2 \phi_p(r) \widehat{f(r)}_q dr \tag{37}$$

$$+ b^2 \sigma(b) \phi_p(b) \int_0^{2\pi} e^{iq\theta} \mathcal{G}_N(\theta) d\theta - a^2 \sigma(a) \phi_p(a) \int_0^{2\pi} e^{iq\theta} \frac{\partial}{\partial r} u(a, \theta) d\theta \tag{38}$$

where $j, p = 0, \ldots, N_r$.

At this stage, we can apply Fourier transform to the integral term having $\mathcal{G}_N$ and the same idea as one-dimensional case to each term about boundary conditions.

# 3 Experiment Results

## 3.1 H/P Convergence Test for Two-dimensional Solution

In this section we present the result of convergence in both $h$ refinement and $p$ refinement with the following steady-state Poisson differential equation:

$$-r^2 \frac{\partial}{\partial r}(\sigma \frac{\partial}{\partial r} u) - r\sigma \frac{\partial}{\partial r} u - \sigma \frac{\partial^2}{\partial \theta^2} u = r \cos\theta \left[ -4r\pi \cos S_r + \{4\pi^2 + 1\} \sin S_r \right], \tag{39}$$

for all $r \in [1, 2], \theta \in [0, 2\pi]$ with $\sigma(r) = r$. The analytic solution is known as

$$u(r, \theta) = \sin S_r \cos\theta, \tag{40}$$

where $S_r = 2\pi(r - 1) - \pi$.

The numerical and exact solutions by the solver we developed is shown in figure (1).

Table 1: This table shows the convergence of h-type (left) and p-type (right) resolution control done above Figure (2). We can see the slopes of each order $P$ is $P + 1$

| Polynomial order | Error($L^\infty$) | Slope |
|---|---|---|
| 5 | $9.3603e-013$ | 5.9406 |
| 6 | $8.6542e-014$ | 6.9402 |

| Element Size | Error($L^\infty$) |
|---|---|
| 0.2 | $1.9385e-012$ |
| 0.1 | $3.4611e-013$ |

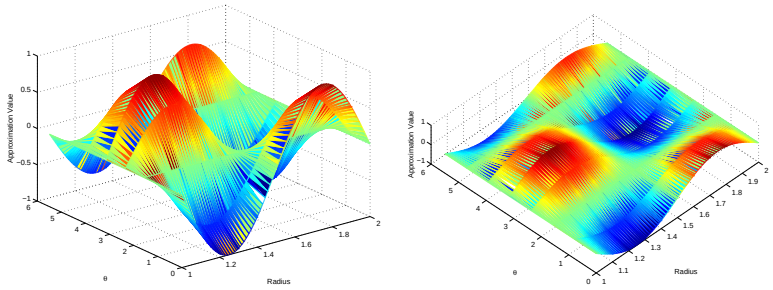


Figure 1: Numerical and exact solution of equation (39) with polynomial order $P = 10$, 10 equidistance elements. This gives the error 4.7740e-15 to the exact solution

### 3.2 High order Polynomial Solution and Its Convergence

In this section we construct a polynomial $P_n$ of order $n$ defined on $[0, 1]$, which satisfies the following.

$$P_n(0) = 0, \quad P_n(1) = 1 \tag{41}$$

$$\frac{d^k}{dx^k}P_n(0) = 0, \quad \frac{d^k}{dx^k}P_n(1) = 0 \tag{42}$$

for all $k = 1, \cdots, n-2$.
Then for each $n$, we obtain a polynomial $P_n$ by solving a system of linear equations having unique solution which determines the set of coefficients of $P_n$. We will apply the spectral polynomial solver to approximate the second derivative $Q_{n-2}$ of $P_n$.

We will investigate the convergences by the h-type, p-type extension of trial functions below.

**Problem 3.1** *Consider the following differential equation for $u(x)$ such that*

$$-r^2\frac{\partial}{\partial r}(\sigma\frac{\partial}{\partial r}u) - r\sigma\frac{\partial}{\partial r}u - \sigma\frac{\partial^2}{\partial\theta^2}u = e^{-(r-1)^2}\{P_n(r) + (2r^2(r-1) - r)P_n'(r) - r^2P_n''(r)\}\cos\theta, \tag{43}$$

*for all $r$ in $[0.1, 1.1]$ with $\sigma(r) = e^{-(r-1)^2}$. Then we have the exact solution as follows.*

$$u(r, \theta) = P_n(r)\cos\theta \tag{44}$$

*where $r$ in $[0.1, 1.1]$ and $\theta$ in $[0, 2\pi]$.*

Note that the accuracy of this interpolation satisfying equations (41) is dependent on the stability of matrix that defines the coefficients of interpolants. We used the Legendre basis function which is known to be more stable than monomials. In spite of this, there exists interpolation error close to $e^{-13}$. This cause the same amount of convergence error in p-type extension mode shown in right of Figure (4) and Table (2).

## 4 Conclusion

Throughout this project, we looked into the theory of Spectral Polynomial and Fourier Method and its solvability. We also investigated the feature of convergence in the viewpoint of h/p convergence

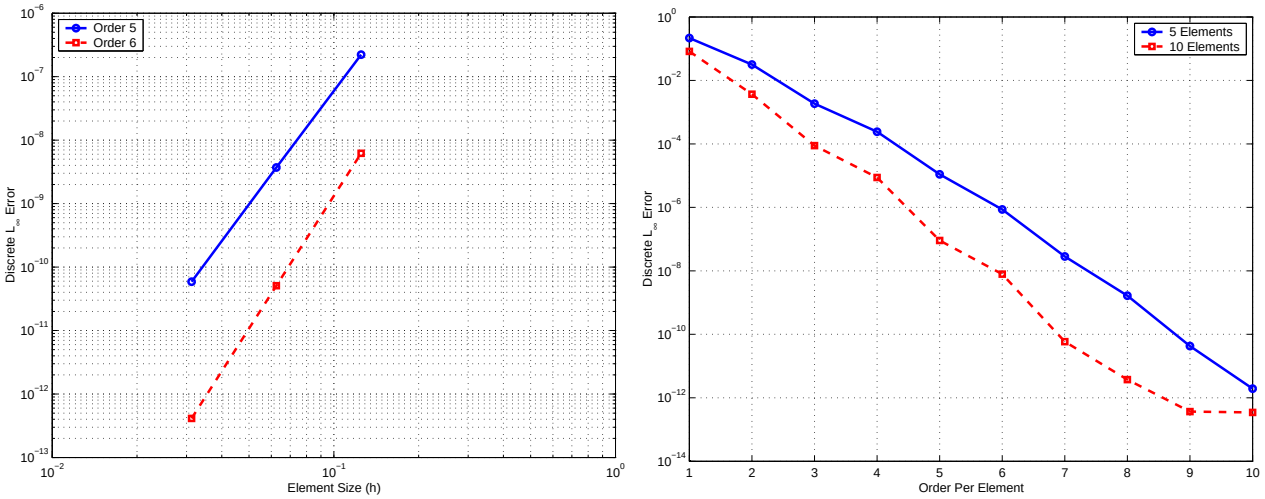


Figure 2: (Left)Convergence with respect to discrete $L^\infty$ norm as a function of size of elements. This test is performed using the h-type extension with fixed polynomial order 5 and 6 respectively. Error on the Log-Log axis is demonstrating the algebraic convergence of the h-type extension. (Right)Convergence w.r.t. $L^\infty$ norm as a function of size of polynomial order in semi-Log plot. It shows the exponential convergence of p-type extension for smooth solution. Two tests are performed for p-type extension with element length 0.2 and 0.1.

Table 2: This table shows the convergence of h-type resolution control done above Figure (4). We can see the slopes of each order $P$ is $P+1$

| Polynomial order | Error($L^\infty$) | Slope |
|---|---|---|
| 5 | $8.5305e-012$ | 5.7556 |
| 6 | $4.7180e-012$ | 6.8332 |

| Element Size | Error($L^\infty$) |
|---|---|
| 0.2 | $9.0616e-13$ |
| 0.1 | $9.4747e-13$ |

property in comparison to classical finite element method. By using Galerkin method, we could incorporate the weak solution and get the problem to be changed to system of linear equations which we can solve it by computer.

By implementing the Spectral element solver for one dimensional Poisson equation having Dirichlet and Neumann boundary conditions, we could experiment all the theory with various specific cases of high-order solutions which were hard to get acceptable convergence in a given time and resolution of domain.

For the future study, we would like deal with problems regarding:

- In supplying $\sigma(r,\theta)$ , we assume $\sigma$ to be dependent only of radius variable. But in general case, we can expand $\sigma$ to be an linear combination of Fourier basis. Computing with only one Fourier basis component, we can easily find the shape of matrix to be dependent of wave number. By adding these matrices up, we could build left hand side stiffness matrix.

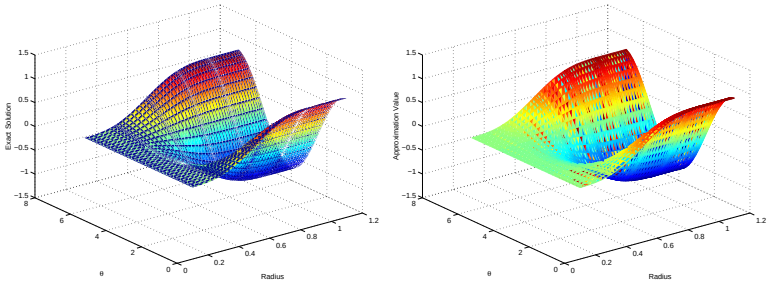


Figure 3: Example of curve that satisfies conditions (41) with polynomial order $n = 7, 9, 12, 14, 15$. The error is $2.9239e - 8$

## References

[1] **Spectral/Hp Element Methods for Cfd**, George Em Karniadakis, Spencer J. Sherwin, Oxford Univ Press, 1999.

[2] **Spectral Methods in MATLAB**, Lloyd N. Trefethen, Society for Industrial and Applied Mathematics, 2001.

[3] **Lecture note of Advanced Methods in Scientific Computing**, Christopher R. Johnson, School of Computing, University of Utah, 2002.

[4] **A direct spectral collocation Poisson solver in polar and cylindrical coordinates**, Chen HL. Su YH. and Shizgal BD., Journal of Computational Physics. 160(2), 453-469 (2000).

[5] **Solving One-dimensional Forward Problems using Spectral Element Method**, S. Choe, Project report in Computational Engineering and Science Program, University of Utah, 2004.

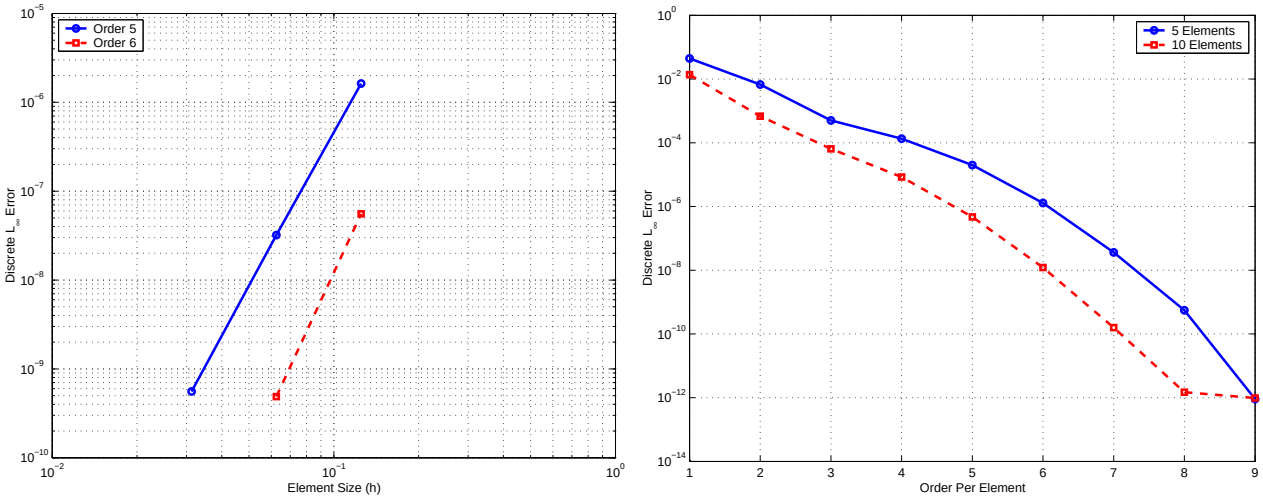


Figure 4: (Left)Convergence with respect to discrete $L^\infty$ norm as a function of size of elements. This test is performed using the h-type extension with fixed polynomial order 3, 4, and 5 respectively. Error on the Log-Log axis is demonstrating the algebraic convergence of the h-type extension. (Right)Convergence w.r.t. $L^\infty$ norm as a function of size of polynomial order in semi-Log plot. It shows the exponential convergence of p-type extension for smooth solution. Two tests are performed for p-type extension with element length 0.2 and 0.1.